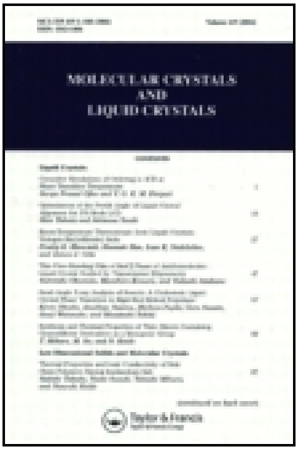

Molecular Crystals and Liquid Crystals

Publication details, including instructions for authors and subscription information:
http://www.tandfonline.com/loi/gmcl20

Multi-Wall Carbon Nanotube Reinforced Thermotropic Liquid Crystal Copolyester Nanocomposites

Hui Jun Choi [a] , Jun Young Kim [b] & Seong Hun Kim [a]

[a] Department of Fiber and Polymer Engineering, Hanyang University, Seongdong-gu, Seoul, Republic of Korea

[b] Material Lab., Corporate R&D Center, SAMSUNG SDI CO., Republic of Korea

Version of record first published: 05 Oct 2009

To cite this article: Hui Jun Choi, Jun Young Kim & Seong Hun Kim (2009): Multi-Wall Carbon Nanotube Reinforced Thermotropic Liquid Crystal Copolyester Nanocomposites, Molecular Crystals and Liquid Crystals, 510:1, 300/[1434]-311/[1445]

To link to this article: http://dx.doi.org/10.1080/15421400903070200

Mol. Cryst. Liq. Cryst., Vol. 510, pp. 300/[1434]–311/[1445], 2009
Copyright © Taylor & Francis Group, LLC
ISSN: 1542-1406 print/1563-5287 online
DOI: 10.1080/15421400903070200

Multi-Wall Carbon Nanotube Reinforced Thermotropic Liquid Crystal Copolyester Nanocomposites

Hui Jun Choi[1], Jun Young Kim[2], and Seong Hun Kim[1]
[1]Department of Fiber and Polymer Engineering, Hanyang University,
Seongdong-gu, Seoul, Republic of Korea
[2]Material Lab., Corporate R&D Center, SAMSUNG SDI CO.,
Republic of Korea

Thermotropic liquid crystal polymer (TLCP) nanocomposites reinforced with a multi-wall carbon nanotube (CNT) were prepared by melt compounding in a twin-screw extruder. The incorporation of CNT has a minor effect on the thermal transition temperatures of TLCP/CNT nanocomposites. The enhancement of thermal stability of TLCP/CNT nanocomposites was obtained by the physical barrier effect of the dispersed CNT in the polymer nanocomposites. There was significant dependence of the rheological and mechanical properties of TLCP/CNT CNT nanocomposites on the CNT contents. The TLCP/CNT nanocomposites exhibited more distinct shear thinning behavior relative to pure TLCP over the whole frequency range, and the non-terminal behavior was observed in the TLCP/CNT nanocomposites attributed to the nanotube-polymer interaction. In addition, the improvement in the mechanical properties of TLCP/CNT nanocomposites can be explained by the reinforcement effect of CNT with high aspect ratio as well as the uniform dispersion of CNT in the TLCP matrix.

Keywords: carbon nanotube (CNT); liquid crystalline polymer (LCP); melt compounding; polymer nanocomposites

INTRODUCTION

Reinforcement of polymer matrix by application of nanomatrial has been an attractive research field in terms of cost effectiveness and performance improvement. Carbon nanotubes (CNTs) have attracted advanced materials, since CNTs were introduced by Iijima in 1991 [1]. Moreover, this discovery has created the practical realization by

Address correspondence to Seong Hun Kim, Department of Fiber and Polymer Engineering, Hanyang University, 17 Haengdang-dong, Seongdong-gu, Seoul 133-791, Republic of Korea. E-mail: kimsh@hanyang.ac.kr

the extraordinary properties of CNTs such as their excellent electrical properties, thermal conductivity, and mechanical strength [2–5]. The fundamental research underlying the applications of CNTs suggests that they can be utilized as a promising reinforcement in new kinds of polymer nanocomposites [6]. The critical issues in development such new composites are improvement of dispersion of CNTs, CNT-polymer interactions, selection of manufacturing process, and cost deduction of the composite. If the cost of CNTs will be on the downward trend, it will be a general material and wide use of the CNT/polymer nanocomposites in the near future.

Thermotropic liquid crystalline polymers (TLCPs) can be oriented to form fibrils under elongational or shear flow. The property results in self-reinforcement in polymer matrix during melt processing [8–9]. Thus, the application of TLCPs for the high performance engineering plastics has attracted researchers [10].

One of the major challenges for high performance polymer nanocomposites is to optimize the processing operations of CNT reinforced polymer nanocomposites with low costs. Various processing techniques have been attempted, including melt compounding, *in situ* polymerization, and solution mixing [11–12]. Of these processing techniques, melt compounding has been accepted as the simplest and most effective method from an industrial perspective, because this process makes it possible to fabricate high performance nanocomposites at low cost, and also facilitates commercial scale up. The combination of a small quantity of expensive CNT with TLCP may provide attractive possibilities to improve the mechanical properties of polymer nanocomposites.

In this research, The amount of CNT incorporated into the TLCP matrix was lowered to $0.5 \sim 2.0\,\mathrm{wt\%}$ to obtain uniform dispersion of CNT in the TLCP matrix. To our conception, attempts to disperse the CNT in the TLCP matrix and to fabricate the TLCP/CNT nanocomposites by melt compounding have not been previously investigated, and the study on the characterization of TLCP/CNT nanocomposites has not yet been reported in the literature. Thus, we would like to clarify the influence on the effect of the CNT on the thermal stability, mechanical properties, and rheological behavior of the TLCP/CNT nanocomposites.

EXPERIMENTAL

The thermotropic liquid crystal polymer used was the wholly aromatic copolyester (Vectra A950, TLCP) with 73 mol% of hydroxy benzoic acid (HBA) and 27 mol% of hydroxyl naphthoic acid (HNA), purchased from

Polyplastics Co., Ltd, (Japan). The nanotubes used were multi-wall CNT (degree of purity >95%) synthesized by a catalytic chemical vapor deposition process, purchased from Iljin Nanotech Co., Korea. The CNT has the diameter of 10~15 nm and the length of 10~20 m.

Preparation of TLCP Nanocomposites

All materials were dried at 120°C *in vacuo* at least 24 hr before use, to minimize the effects of moisture. The TLCP/CNT nanocomposites were prepared by a melt compounding in a Haake rheometer (Haake Technik GmbH, Germany) equipped with a twin-screw. The temperature of the heating zone, from the hopper to the die, was set to 290, 315, 320, and 300°C, and the screw speed was fixed at 30 rpm. For the fabrication of TLCP/CNT nanocomposites, TLCP was melt blended with the addition of various CNT content, specified as 0.5, 1.0, and 2.0 wt% in the polymer matrix, respectively.

Characterization

Thermal properties of the TLCP/CNT nanocomposites was performed with a TA Instrument 2010 differential scanning calorimetry (DSC) over the temperature range of 30~300°C at heating and cooling rate of 10°C/min. Thermogravimetric analysis (TGA) of the TLCP/CNT nanocomposites was performed with a PerkinElmer Pyris-1 over the temperature range of 30~900°C at a heating rate of 10°C/min under nitrogen atmosphere. The rheological properties of the TLCP/CNT nanocomposites as a function of angular frequency were measured at 310°C with an advanced rheometric expansion system (ARES) rheometer (Rheometric Scientific, Inc.). The mechanical properties of the TLCP/CNT nanocomposites were measured at room temperature using an Instron 4465 testing machine, according to the procedures in the ASTM D 638 standard. The gauge length and the crosshead speed were set to 20 mm and 10 mm/min, respectively. The morphology of the TLCP/CNT nanocomposites was observed using a JEOL JSM-6340 F scanning electron microscope (SEM). The texture of TLCP/CNT nanocomposites was identified with an Olympus BX51 polarizing optical microscope.

RESULT AND DISCUSSION

Thermal Behavior

The effect of CNT on the thermal properties of the TLCP/CNT nanocomposites was characterized by means of DSC analysis. DSC cooling

TABLE 1 Thermal Behavior of the TLCP/CNT Nanocomposites with CNT Content

Materials	$T_c{}^a$ (°C)	$T_{kn}{}^b$ (°C)	$T_i{}^c$ (°C)	$T_{max}{}^d$ (°C)	A^*	K^*	*IPDT*	$W_R{}^e$ (%)
TLCP	239.7	280.5	491.5	507.3	0.81	2.09	1338.0	52.3
TLCP/CNT 0.5	237.5	278.5	494.0	516.3	0.81	2.08	1338.6	52.6
TLCP/CNT 1.0	237.3	278.6	496.3	517.3	0.82	2.12	1366.9	53.7
TLCP/CNT 2.0	236.9	277.7	495.0	510.8	0.82	2.17	1400.6	54.0

[a] The crystallization temperature in DSC at a cooling at 10°C/min.

[b] The crystalline to nematic temperature in DSC at a heating rate of 10°C/min.

[c] Initial decomposition temperature in TGA at a heating rate of 10°C/min.

[d] Decomposition temperature at the maximum decomposition rate.

[e] Rasidual yield in TGA at 600°C.

and heating data of the TLCP/CNT nanocomposites with the CNT content are shown in Table 1. The presence of CNT within the TLCP matrix has a minor effect on the crystallization and transition temperatures of the TLCP/CNT nanocomposites.

TGA thermograms of the TLCP/CNT nanocomposites with the CNT content at a heating rate of 10°C/min under a nitrogen atmosphere are shown in Table 1. It can be seen that the decomposition temperatures and the residual yield of the TLCP/CNT nanocomposites were increased with increasing CNT content. The incorporation of CNT into the TLCP matrix may retard the rate of thermal decomposition in the polymer nanocomposties, resulting in the enhancement of thermal stability of the TLCP/CNT nanocomposites. The improved thermal stability of TLCP/CNT nanocomposites is associated with the interaction between TLCP and CNT. The decomposition temperature including initial decomposition temperature (T_i), thermal decomposition temperature at the maximum rate (T_{max}), and residual yield (W_R) of the TLCP/CNT nanocomposites increased with increasing CNT content, indicating the thermal decomposition of the TLCP/CNT CNT nanocomposites was retarded by incorporating CNT into the TLCP matrix. In addition, the residual yields of the TLCP/CNT nanocomposites increased with increasing CNT content, indicating that the thermal decomposition of the polymer matrix was retarded in the TLCP/CNT nanocomposites with higher residual yield.

Based on the Doyle's proposition [13], the integral procedural decomposition temperature (*IPDT*) of the TLCP/CNT nanocomposites can be determined from TGA curves according to the following equations [14], and the results are shown in Table 1.

$$IPDT\ (^\circ\mathrm{C}) = A^*K^*(T_f - T_i) + T_i$$

$$A^* = \frac{A1 + A2}{A1 + A2 + A3} \quad \text{and} \quad K^* = \frac{A1 + A2}{A1}$$

where, A^* is the ratio of the area of TGA curve up to the temperature divided by that of the total TGA curves; K^* is the coefficient of A^*; T_i is the initial experimental temperature, and T_f is the final experimental temperature. As shown in Table 1. The values of *IPDT*, A^*, and K^* for the TLCP/CNT nanocomposites were increased with increasing CNT content. This result means that the incorporation of CNT into the TLCP matrix enhanced the thermal stability of the TLCP/CNT nanocomposites. The improvement in the thermal stability of the TLCP/CNT nanocomposites may be explained by the fact that the dispersed CNT in the polymer nanocomposites can act as physical barriers which retard the decomposition rate and prevent the diffusion-out of volatile decomposed products in the polymer nanocomposites, resulting in the increased thermal stability of the TLCP/CNT nanocomposites [15].

Rheological Behavior

The complex viscosity ($|\eta^*|$) of pure TLCP and the TLCP/CNT nanocomposites at 310°C as a function of frequency are shown in Figure 1. The $|\eta^*|$ of the TLCP/CNT nanocomposites decreased with

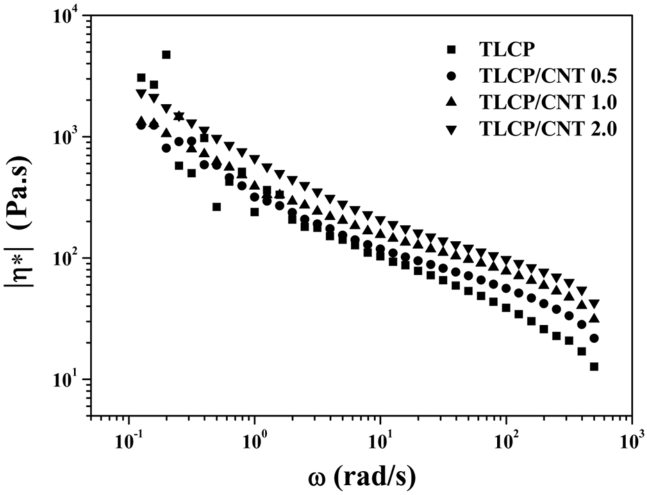

FIGURE 1 Variation of complex viscosity of the TLCP/CNT nanocomposites with CNT content measured at 310°C.

increasing frequency, indicating that the TLCP/CNT nanocomposites exhibited shear thinning behavior over the whole frequency range investigated, due to the random orientation of rigid rod-like molecular chains by shear forces. The increase in the $|\eta^*|$ of TLCP/CNT nanocomposites with increasing CNT content was more significant at low frequency region rather than at high frequency region. This effect was reduced with increasing frequency because of the strong shear thinning behavior induced by incorporating CNT. As $|\eta^*|$ of the TLCP/CNT nanocomposites increased with increasing CNT content, and this could be attributed to the physical interactions between the nanotube-polymer [4,16]. This phenomenon was related to the increase storage modulus (G') of TLCP/CNT nanocomposites with increasing CNT content.

The variations of storage modulus (G') and loss modulus (G'') of the TLCP/CNT nanocomposites as a function of frequency are shown in Figure 2. The values of G' and G'' of the TLCP/CNT nanocomposites were increased with increasing frequency and CNT content. In addition, G' and G'' of the TLCP/CNT nanocomposites were higher than those of pure TLCP and increased with increasing CNT content. Those phenomena were similar to the tendency observed in the $|\eta^*|$ of the TLCP/CNT nanocmoposites with increasing CNT content. The storage modulus of TLCP/CNT nanocomposites increased with increasing frequency and was higher than that of pure TLCP. The storage modulus of the TLCP/CNT nanocomposites increased with increasing CNT content. This result can be explained the fact that the physical interaction between the nanotubes could lead to the formation of an interconnected or network-like structures of the nanotubes in the TLCP matrix as the CNT content increased [17]. And also this result was similar to the tendency observed in the complex viscosity of TLCP/CNT nanocomposites with increasing CNT contents.

In addition, the TLCP/CNT nanocomposites exhibited more distinct shear thinning behavior relative to pure TLCP over the whole frequency measured, and the non-terminal behavior observed in the TLCP/CNT nanocomposites was attributed to the nanotube-polymer interaction [18,19].

The shear thinning exponent and relaxation exponent of the TLCP/CNT nanocomposites were characterized to investigate the effect of CNT of the rheological properties of TLCP/CNT nanocomposites. The shear thinning exponent can be calculated from the slope of complex viscosity versus frequency, and the relaxation exponent is the slope of storage modulus versus frequency [20,21]. An ideal non-Newtonian fluid has a shear thinning exponent that equals or approaches zero, and the viscosity is independent of frequency.

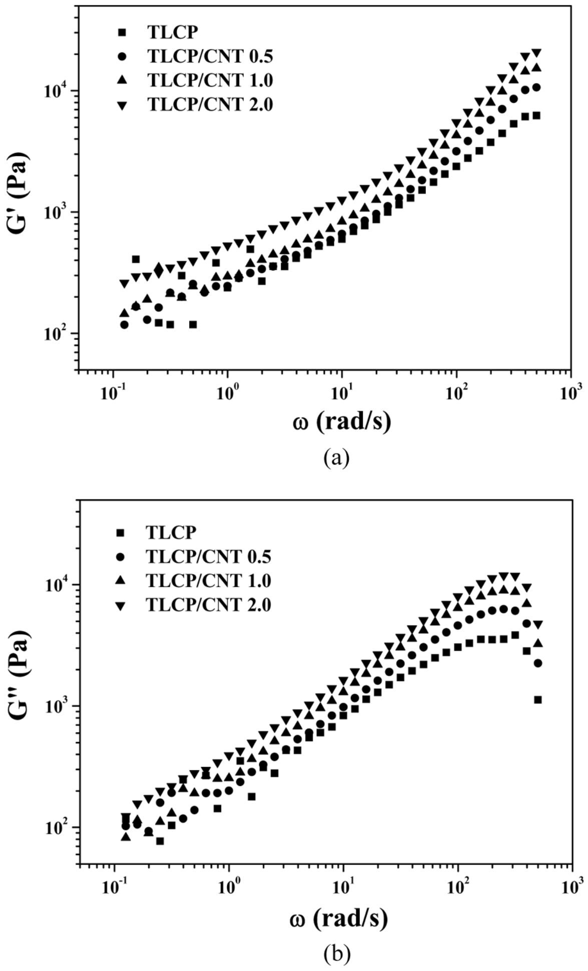

FIGURE 2 Variation of (a) storage modulus and (b) loss modulus of the TLCP/CNT nanocomposites with CNT content as a function of frequency.

The shear thinning exponent and relaxation exponent of TLCP/CNT nanocomposites, determined by fitting of the experimental data at low frequency to power-law equations, such as complex viscosity $\approx \omega^n$ and storage modulus $\approx \omega^n$ [20], are shown in Table 2. Many researches have reported that the shear thinning behavior significantly depends on the filler content in polymer/filler composites [20–22]. The shear thinning exponent values of the TLCP/CNT nanocomposites decreased with increasing CNT content, indicating that shear thinning behavior of the TLCP/CNT nanocomposites

TABLE 2 The Shear Thinning Exponent and Relaxation Exponent of the TLCP/CNT Nanocomposites with CNT Content

Materials	Shear thinning exponent (n)	Relaxation exponent (n)
TLCP	−0.44	0.43
TLCP/CNT 0.5	−0.51	0.38
TLCP/CNT 1.0	−0.53	0.36
TLCP/CNT 2.0	−0.56	0.35

significantly depended on CNT content. The relaxation exponent of TLCP/CNT nanocomposites decreased with increasing CNT content, and the extent of decrease was more distinct at higher CNT content. This was attributed that nanotube-nanotube interactions dominate with increasing CNT content, leading to the formation of an interconnected structure or network-like of CNT in the TLCP/CNT nanocomposites. This result suggests that the incorporation of CNT leads to more rigid and stiffer polymer chains in the TLCP/CNT nanocomposites, resulting in the increase in the relaxation exponent for the flow process [16,23–24].

Mechanical Properties

The variation of stress-strain curves of the TLCP/CNT nanocomposites with the CNT contents is shown in Figure 3. The tensile strength and modulus were calculated average from the stress-strain profiles and are shown in Table 3. The addition of CNTs into the TLCP matrix improved the tensile strength and modulus of the TLCP matrix. There is a significant dependence of the mechanical properties of the TLCP/CNT nanocomposites of the CNT content. Addition of CNT to TLCP matrix increased the tensile modulus and strength and decreased the elongation at break. The tensisle strength and modulus of TLCP/CNT nanocomposites increased from 62.3 in pure TLCP to 89.3 MPa (an increase of 43.3%) and 1.12 to 1.79 GPa (an increase of 59.8%), respectively, when the CNTs content reached 2 wt% in TLCP/CNT nanocomposites. When the CNTs loading is increased, the elongation at break of the TLCP/CNT nanocomposites is reduced that the TLCP/CNT nanocomposites were more brittle and stiff with the incorporation of the CNT. The incorporation of CNT improved the mechanical properties of the TLCP/CNT nanocomposites due to the reinforcement effect of the CNT with high aspect ratio, their uniform dispersion in the TLCP matrix, and this improvement being more significant at lower CNT content. However, mechanical properties of the TLCP/CNT nanocomposites are improved but not enough as

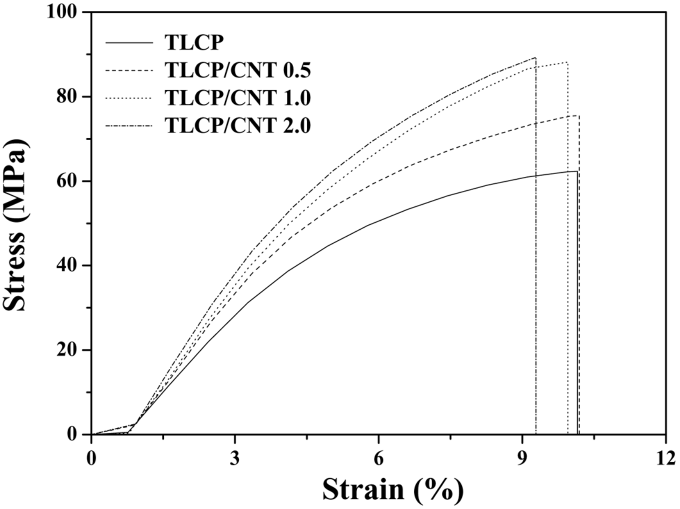

FIGURE 3 Stress-strain curves of the TLCP/CNT nanocomposites with CNT content.

expected. The reason is weak bonding between the CNT and the surrounding TLCP matrix. As the interfacial bonding between the CNTs and the polymer matrix is weak, the CNT often tends to from bundles together due to intrinsic van der Waals attraction between the individual nanotubes in combination with high aspect ratio and large surface area of the CNT, and leading to some agglomeration [25]. Thus prevent an efficient load transfer to the polymer matrix.

Morphology

The morphologies of the TLCP/CNT nanocomposites are shown in Figure 4. As shown in Figure 4(a), the TLCP/CNT nanocomposites

TABLE 3 The Mechanical Properties of the TLCP/CNT Nanocomposites with CNT Content

Materials	Tensile strength (MPa)	Tensile modulus (GPa)	Elongation at break (%)
TLCP	62.3	1.12	10.15
TLCP/CNT 0.5	75.5	1.57	10.18
TLCP/CNT 1.0	88.2	1.60	9.95
TLCP/CNT 2.0	89.3	1.79	9.26

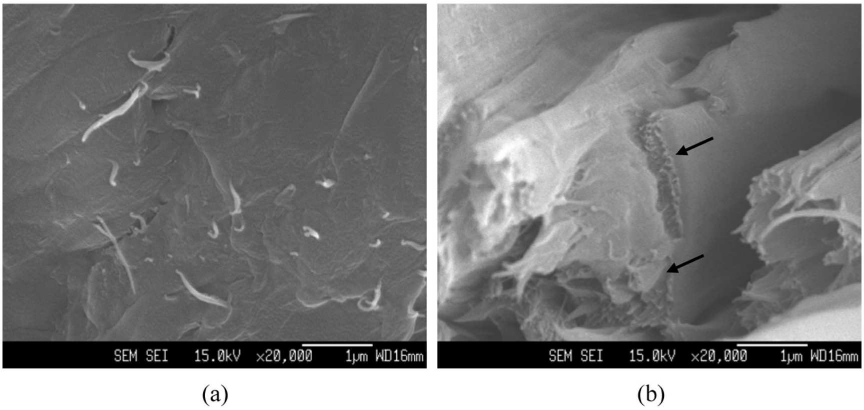

FIGURE 4 SEM microphotographs of TLCP/CNT nanocomposites at (a) 0.5 wt% and (b) 2.0 wt% CNT content.

exhibited a uniform dispersion of the CNTs in the TLCP matrix, in comparison with the nanocomposites with higher CNT contents. At higher CNT content, less uniformly dispersed and more agglomerated of CNT were formed in the TLCP matrix, as shown in Figure 4(b). As a result, the tensile strength of the TLCP/CNT nanocomposites was not increased significantly at high CNT content, as expected, compared with that at low content, resulting form some agglomerates of randomly dispersed CNT in the polymer nanocomposites. Therefore, to achieve further enhanced mechanical properties of the TLCP/CNT nanocomposites, the improvement on both the dispersion of CNT in the TLCP matrix and in the interfacial interaction between the CNT

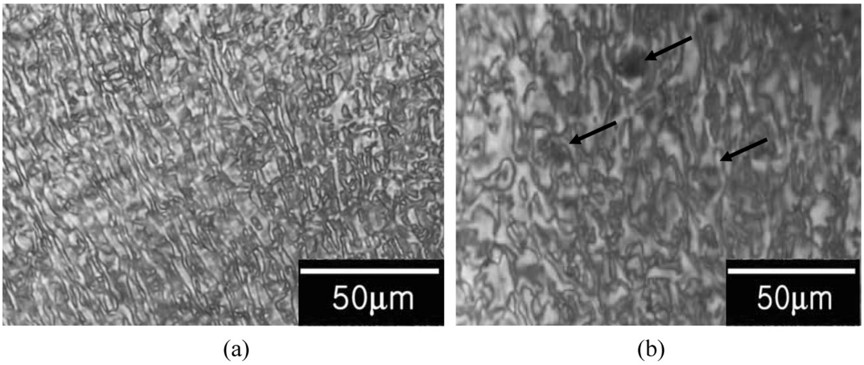

FIGURE 5 Optical micrographs of the TLCP/CNT nanocomposites at 280°C; (a) Pure TLCP and (b) 2.0 wt% CNT content.

and TLCP matrix through functionalization of CNTs should be required, and our recent research is also aimed at that topic.

To analyze the liquid crystalline behavior, TLCP/CNT nanocomposites was employed polarize optical microscope. It is clear from the Figure 5(a and b) that thread and droplet structure can be seen in these images, which are the representative structure of nematic liquid crystals. The presence of CNT within the TLCP matrix increased droplet structure size on the liquid crystal phase and the overall thread structure decreased.

CONCLUSIONS

The TLCP/CNT nanocomposites were prepared by simple melt compounding in a twin-screw extruder. The increase in the thermal decomposition temperatures and the residual yield of the TLCP/CNT CNT nanocomposites with increasing CNT content indicated that the incorporation of a small quantity of CNT could improve the thermal stability of the TLCP/CNT nanocomposites, resulting from the effective function of CNT as physical barriers to prevent hinder the transport of thermal energy in the TLCP/CNT nanocomposites during thermal decomposition. There was significant dependence of the rheological and mechanical properties of the TLCP/CNT nanocomposites on the CNT content. The TLCP/CNT nanocomposites exhibited more distinct shear thinning behavior as compared to pure TLCP over the whole frequency measured. The storage and loss moduli the TLCP/CNT nanocomposites increased with increasing frequency and CNT content, and this enhancement effect was more pronounced at low frequency than at high frequency. As the CNT content increased, the terminal zone slopes of G' for the TLCP/CNT nanocomposites were decreased, and the non-terminal behavior observed in the TLCP/CNT nanocomposites was related to the nanotube-polymer interaction, leading to the formation of the interconnected or network-like structures of CNT in the polymer nanocomposites. The tensile strength and tensile modulus of the TLCP/CNT nanocomposites were improved with increasing CNT content due to the reinforcement effect of CNT with high aspect ratios as well as good dispersion of CNT in the TLCP matrix, and this enhancing effect was more significant at low CNT content than at high CNT content.

REFERENCES

[1] Iijima, S. (1991). *Nature*, *354*, 56.
[2] Iijima, S. & Ichihashi, T. (1993). *Nature*, *363*, 603.

[3] Yu, M. F., Files, B. S., Arepalli, S., & Ruoff, R. S. (2000). *Phys. Rev. Lett.*, *84*, 5552.
[4] Kim, J. Y. & Kim, S. H. (2006). *Polym, J. Sci. Part B: Polym. Phys.*, *44*, 1062.
[5] Kim, J. Y., Han, S. I., & Kim, S. H. (2007). *Polym. Eng. Sci.*, *47*, 1715.
[6] Antonucci, V., Hsiao, K. T., & Advani, S. G. (2003). In: *Advanced Polymeric Materials: Structure Property Relationships*, Shonaike, G. O. & Advani, S. G. (Eds.), CRC Press: New York, Ch. 11, 397–437.
[7] Odom, T. W., Huang, J. L., Kim, P., & Lieber, C. M. (1998). Atomic structure and electronic properties of single-walled carbon nanotubes. *Nature*, *391*, 59–62.
[8] Chung, T. S. (1986). *Ploymer. Eng. Sci. R*, *41*, 1.
[9] Bretas, R. E. S. & Baird, D. G. (1992). *Polymer*, *33*, 5233.
[10] Kim, J. Y. & Kim, S. H. (2005). *J. Polym. Sci. Part B: Polym. Phys.*, *43*, 3600.
[11] Haggenmuller, R., Conmas, H. H., Rinzler, A. G., Fischer, J. E., & Winey, K. I. (2000). *Chem. Phys. Lett.*, *330*, 219.
[12] Jia, Z. J., Wang, Z. Y., Liang, J., Wei, B. Q., & Wu, D. H. (1999). *Mater. Sci. Eng. A*, *271*, 395.
[13] Doyle, C. D. (1961). *Anal. Chem.*, *33*, 77.
[14] Park, S. J. & Cho, M. S. (2000). *J. Mater. Sci.*, *35*, 3525.
[15] Kashiwagi, T., Shields, E. J. R., Harris, R. H., & Davis, R. D. (2003). *J. Appl. Polym. Sci.*, *87*, 1541.
[16] Kim, J. Y., Park, H. S., & Kim, S. H. (2007). *J. Appl. Polym. Sci.*, *103*, 1450.
[17] Potschke, P., Fornes, T. D., & Paul, D. R. (2002). *Polymer*, *43*, 3247.
[18] Rosedalev, J. H. & Bates, F. S. (1990). *Macromolecules*, *23*, 2329.
[19] Larson, R. G., Winey, K. I., Patel, S. S., Watanabe, H., & Bruinsma, R. (1993). *Rheol. Acta*, *32*, 245.
[20] Costa, F. R., Wagenknecht, F. R. U., Jehnichen, D., Abdel-Goad, M., & Heinrich, G. (2006). *Polymer*, *47*, 1649.
[21] Wagener, R. & Reisinger, T. J. G. (2003). *Polymer*, *44*, 7513.
[22] Krishnamoorti, R., Vaia, R. A., & Giannelis, E. P. (1996). *Chem. Mater.*, *8*, 1728.
[23] Costa, F. R., Wagenknecht, U., Jehnichen, D., Abdel-Goad, M., & Heinrich, G. (2006). *Polymer*, *47*, 1649.
[24] Wagener, R. & Reisinger, T. J. G. (2003). *Polymer*, *44*, 7513.
[25] Ebbesen, T. (1997). *Carbon Nanotubes: Preparation and Properties*, CRC Press: New York.